THE EFFECT OF MATERIAL STRAIN HARDENING ON THE BUCKLING STRENGTH OF A PERFORATED PLATE UNDER UNIAXIAL LOADING

by

MAYURI SURESH PATIL

Presented to the Faculty of the Graduate School of

The University of Texas at Arlington in Partial Fulfillment

of the Requirements

for the Degree of

MASTER OF SCIENCE IN MECHANICAL ENGINEERING

THE UNIVERSITY OF TEXAS AT ARLINGTON

December 2015

Acknowledgements

It is a genuine pleasure to express my deep sense of thanks and gratitude to my mentor and guide Dr. Kent L. Lawrence. I am indebted to him for his constant support and patients through my thesis. His timely advice and scientific approach has helped me to a great extent to accomplish my task.

I would like to thank Dr. Wen S. Chan and Dr. Bo P. Wang for their invaluable time to serve on my committee.

Also I would like to thank the Mechanical & Aerospace Engineering Department for all the help made available to me.

Most importantly I would like to thank my parents for their unbound support and my brother Mr Viraj Patil for being so interested with my work. I would like to dedicate my thesis to my mother Ms Sumedha S. Patil and my father Mr Suresh V. Patil

November 4, 2015.

Abstract

THE EFFECT OF MATERIAL STRAIN HARDENING ON THE BUCKLING STRENGTH OF A PERFORATED PLATE UNDER UNIAXIAL LOADING

Mayuri Suresh Patil, MS

The University of Texas at Arlington, 2015

Supervising Professor: Kent L. Lawrence

Plates or members containing plate elements have been used in the offshore, aerospace and construction industry. Cutouts are often located to lighten the weight of the structure, but these cutouts reduce the ultimate strength of the plate.

A number of studies have taken place for determining the buckling strength of a perforated plated but few discuss the effect of material strain hardening on the buckling strength of a perforated plate.

Buckling strength is often considered as an important criterial to determine the serviceable limit of the perforated plate in structures. The aim of the present study is to investigate the effect of material strain hardening on the strength characteristic of a perforated plate under uniaxial loading. This load at some point could lead to a possibility of instability.

For this study a square plate with perforation is considered here. The plate is considered to be simply supported at all four edges and has been kept straight. The perforation is located at the center of the plate. A number of ANSYS FEM static nonlinear analyses are undertaken with different strain hardening material properties for AL7075. The Ramberg-Osgood method is used to determine the non-linear stress-strain curve for different strain hardening values. The plate thickness and the diameter of the cutout are

varied to determine the effect on the strength. The study covers the behavior of the system in both the elastic buckling region and the elastic-plastic region.

Table of Contents

List of Illustrations

List of Tables

CHAPTER 1

INTRODUCTION

1.1 Introduction

Plates are considered an important structural component in structures like ships, bridges, aerospace structure, off shore structures, etc. At times the presence of a perforation in a plate element is used for inspection, maintenance and service purposes. The size of these perforations have a large influence on the strength of the plate. The presence of a perforation re-distributes the plate membrane stresses in turn reducing the strength of the structure.

Plates subjected to uniaxial, biaxial, shear or combined loadings makes the plate unstable at some point, which causes the plate to buckle. Buckling of such structure is used as the serviceable limit for plate design purpose. Buckling occurs when a structure undergoes evidently large visible deflection in the transverse direction.

The buckling of a system could be due to global buckling of the entire structure, local buckling, couple buckling etc. Hence it becomes important to study the local buckling, i.e. buckling at the individual plate element level.

When the plate is slender, the plate buckles within the material elastic limit. As the plate becomes thick and stiff, buckling takes place in the elastic-plastic region. For such cases a certain degree of plasticity is always attained before the initiation of buckling. Buckling in the plate is seen after the load exceeds the critical load for such cases. The plate will suddenly bend after reaching the critic load.

1.2 Literature Survey

The buckling of a perforated plate has been the main focus in many studies. The studies are for elastic buckling and plastic buckling.

Mauro Real and Liercio Isoldi [1] have done an FEM analysis for a square and rectangular steel plate with perforation under uniaxial compressive loading for material failure. The study concluded that for thin plates, the instability occurs at average stress, which is the elastic buckling. While buckling of thick plates with large hole may occur after the material reaches the yield limit, which is in the plastic buckling range.

The study by EL-Sawy and Namy [2] investigated the effect of perforation size, the perforation location, slenderness ratio of the plate and the yield point using different grades of steel for square and rectangular plates under uniaxial compressive loading to determine the behavior of critical buckling stress using the FEM analysis. The study concluded by recommending some sizes of perforation for different thickness and the location of perforation for different plate thicknesses and aspect ratios.

Maarefdoust and Kadkhodayan [3] did an analysis for elastoplastic buckling behavior of thick plates under uniaxial, biaxial compression, pure shear and combined loading using generalized differential quadrature method. They also used incremental (IT) and deformation (DT) theories of plasticity to develop non-linear equilibrium equations. The strain hardening effect for materials was considered by using the Ramberg-Osgood formulation [9]. The study concludes by giving a comparison of IT and DT method used for theoretical calculation in the plastic region.

Author Paik [4] explains the ultimate strength behavior of the perforated steel plate under combined biaxial compression and edge shear loading. The analysis is done in FEM.

Closed form of empirical formulas for stability were derived for the ultimate strength of a perforated plate under combined loading on the basis of the ANSYS FEM results.

The study by Brown and Yettram [5] discussed elastic stability of perforated plates using the conjugate load method. The cases are for different loading and support conditions. They conclude that the conjugate load method of instability could be used for perforated plates.

Durban and Zuckerman [6] investigated the elastoplastic buckling behavior of a rectangular plate with different boundary conditions. The plate is subjected to uniform compression load along with tension load. The analysis is based on two methods, standard linear buckling equation and the deformation theory of plasticity. Here for a set of boundary conditions an optimal loading path for critical buckling is described.

In the journal paper by Shakerlry and Brown [7], a conjugate load/displacement method is implemented on a square plate with a perforation. The perforation considered was a rectangular shape geometry. This plate undergoes uniaxial and shear loading conditions for simply supported and fixed boundary conditions. The study results in a design guideline for the location of the perforation.

The remaining chapters in this thesis discuss the theory of elastic buckling, stress strain curves in the plastic region and the software implementation for buckling analysis.

1.3 Problem Description

From the literature survey it was evident that a number of studies have taken place to determine the buckling strength of a perforated plate. Further studies have also been done to determine the appropriate size of the perforation and its location. But during these studies, the material of the plate elements were assumed to follow the elastic-perfectly plastic scheme, i.e., by ignoring the strain hardening effect on the system to reduce the complications. The present study considers the strain hardening effect on the buckling strength of perforated plates.

Initially a verification of computational modeling is done by comparing the results with the references [1][2][3], which is discussed briefly in the next chapters. Then the implementation of the strain hardening is performed for the various cases.

A plate of 1000x1000mm is considered in this study. The plate has a circular shaped perforation at its center. This plate is modeled in Creo. The plate is considered to have an average level of initial imperfection. This initial imperfection in the plate occurs during welding fabrication. The depth of this imperfection could be estimated by b/2000, where ‘b’ is the plate width. The shape of this imperfection is determined from linear buckling mode obtained from the perfect plate. For the square plate considered the imperfection shape would be a half wave as shown in Figure 1-1.

The plate is simply supported on all the four edges and is subjected to axial compressive force along two parallel edges. The ANSYS static-nonlinear simulations are conducted for various slenderness ratios, perforation size and strain hardening curves. Plate critical buckling loads are calculated for different strain hardening curves and for

different slenderness ratios. The following chapters provide a detail study of the mesh convergence, boundary settings, material settings and the output results.

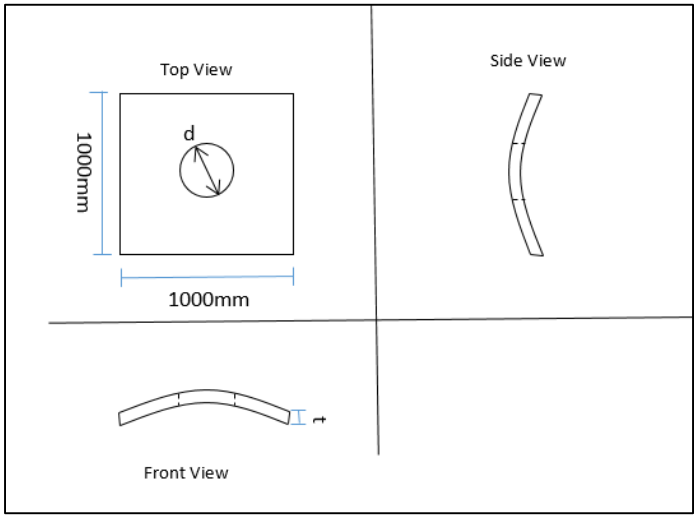

Figure1-1 Geometric sketch of a plate with initial imperfection. (Here, d = perforation diameter, t = thickness of the plate)

CHAPTER 2

PLATE BUCKLING THEORY

2.1 Introduction

Buckling of plates is nothing but the out of plane sudden deformation seen in plates due to a highly unstable compressive stress. The load at which the plate buckles is called the critical buckling load or the stress at that point is called the critical buckling stress. The shape of buckling depends upon the load and support conditions.

This study focuses on local buckling. Suppose an assembly is made up of thin plate cross-sections. When this assembly undergoes a large compressive stress, the thin plate that make up the assembly may buckle before the full strength of the member is achieved. This buckling could be because the plates are not perfectly planar, loads are not perfectly aligned and materials are not perfectly isotropic and homogeneous. And when one of the cross-section member fails in buckling then the member capacity is reached. This is nothing but local buckling.

Figure 2-1 Example for local buckling [13]

There are two type of buckling discussed in this chapter,

i) Elastic buckling- occurs for slender and thin walled plates

ii) Plastic buckling- It occurs when the plate is thick.

2.2 Elastic Buckling

The buckling of the plate is elastic when the plate thickness is small with respect to lateral dimensions ‘a’ and ‘b’. Timoshenko [8] explains the theoretical calculations to obtain the critical load applied in the middle plane of the plate. It is assumed that the plate initially has some initial curvature or lateral loading.

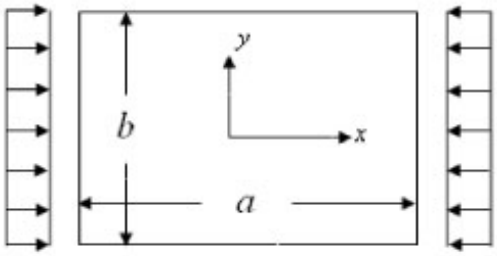

Figure 2-2 Slender plate under uniaxial loading in ‘x’ direction

The formula for calculating the critical load of buckling for uniaxial loading and simply supported boundary condition case is [8],

$$Ncr = \frac{\pi^2 D}{a}\left(m + \frac{1}{m}\frac{a^2}{b^2}\right)^2$$

Where,

N_{cr} = Critical Buckling Load

D = Flexural rigidity of the plate,

$$D = \frac{E\,t^3}{12(1 - Nu^2)}$$

Here ‘*t*’ is the thickness of the plate, ‘*E*’ is the young’s modulus and ‘*Nu*’ is the possion’s ratio.

a ,*b* = are the length and the breath of the rectangular plate.

m = Number of half waves into which the plate buckles.

The critical buckling stress σ_{cr} could be obtained by further by,

$$\sigma cr = \frac{Ncr}{b \times t}$$

These calculations are valid for plates without perforations. As there is no analytical solution available for buckling of perforated plates; the approach adopted for such cases are eigenvalue buckling analysis.

It is seen that for thin plate made up of material of yield stress of σ_y, instability occurs at stress σ_{cr}. Here for the elastic buckling which takes place in the linear region the value of σ_{cr} would be much lesser than the σ_y. Especially for plate without perforation.

2.3 Plastic Buckling

It is difficult to adopt the above method for determining the critical load in the plastic region . As the initial stress stiffness matrix is not proportional to the stress level in the plate anymore due to geometric and material non-linearity. Hence the analysis for buckling in the plastic region is done using FEM software's.

For thick plates or plates with large holes, it is seen that the plate material reaches the yield point at some portions of the plate causing it to buckle elasto-plastically. But if the material thickness is comparatively large then the material failure may occur before any considerable buckling takes place.

CHAPTER 3

STRAIN HARDENING

It is a process of making the metal harder and stronger through plastic deformation. In this the specimen is put through cold-working and heated at a relatively low temperature. The strength of the metal is increased but the ductility decreases.

3.1 Ramberg-Osgood Plastic stress-strain curve.

The Ramberg-Osgood equation was created to describe the non-linear relationship between the stress and the strain. Especially useful for metals that harden with plastic deformation.

$$\varepsilon = \frac{\sigma}{E} + \frac{k\,\sigma 0}{E}\left(\frac{\sigma}{\sigma 0}\right)^{c}$$

Where, *ε* - total plastic strain,

σ - stress,

E - young's modulus

σ0 - yield strength, and

k and *c* are material parameters describing the hardening behaviour.

Here the first part of the equation *(σ/E)* defines the elastic part of strain while the other term $\left[\frac{k\,\sigma 0}{E}\left(\frac{\sigma}{\sigma 0}\right)^{c}\right]$ describes the plastic non-linear behavior.

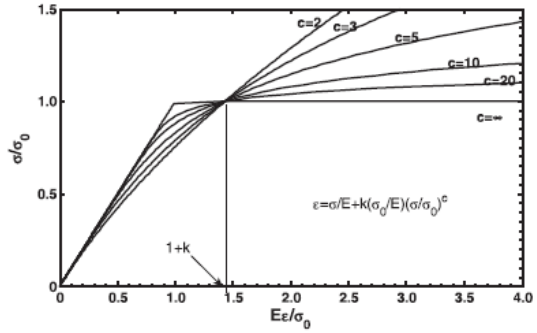

Figure3-1 Ramberg-Osgood stress-strain relationship [3]

Figure 3-1 describes the stress strain curve obtained for different exponential values '*c*'.

3.1.1 Stress Strain relationship for AL7075-T6

The Ramberg-Osgood equation provided above, is used to calculate the curve for Aluminum grade AL7075-T6. Figure 3-2, depicts the stress strain curve for three exponential values of c = 5, 10 and 20.

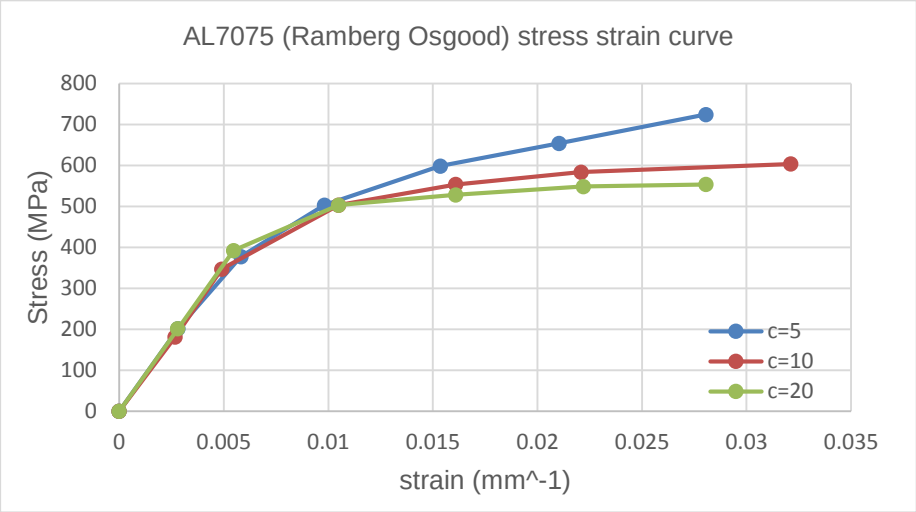

Figure 3-2 AL7075 (Ramberg - Osgood) stress strain curve

For the present study these stress strain curves are provided to the software in piecewise linear segment to follow the nonlinear behavior of the material.

CHAPTER 4

VERIFICATION OF METHOD OF ANALYSIS

In order to verify the method of analysis used in this study, a comparison with the existing results in the literature on the elastic and elastoplastic buckling were performed. The results by Mauro Real, Liercio Isoldi [1], EL-Sawy and Namy [2] and Maarefdoust and Kadkhodayan [3] were used for this purpose.

The first case of simulation were to study the elastic and plastic buckling of the plate using the work of, Mauro Real, Liercio Isoldi [1] and EL-Sawy and Namy [2]. While the second set of simulations were to compare the buckling results for Ramberg-Osgood stress strain curve used by the author Maarefdoust and Kadkhodayan [3].

4.1 Computational verification for elasto-plastic buckling

For first verification of computational modeling, the critical load of a non-perforated plate was numerically evaluated and the results were compared to the analytical solutions.

4.1.1 Plate without perforation

4.1.1.1 Overview

A compressive plate simply supported on all four edges was subjected to uniaxial loading along the short edge. The plate was meshed with 8-node shell elements.

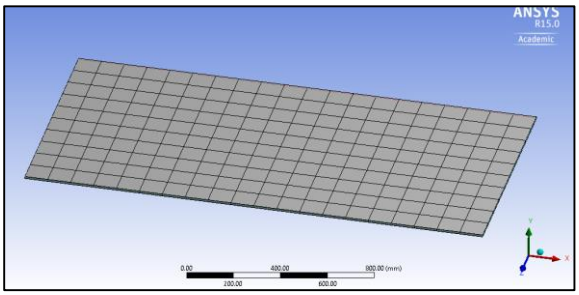

Figure 4-1 Plate without hole with 200 shell elements

4.1.1.2 Simulation results

The numerical results for critical linear elastic buckling load obtained were **735 KN/m** .

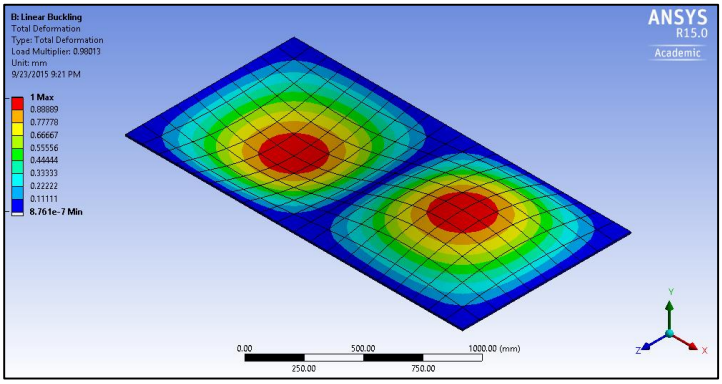

Figure 4-2 Plate buckling

4.1.1.3 Comparison of results.

The buckling load obtained for our case is **735kN**

i) Comparing the obtained value with the theoretical value,

Theoretical Buckling Load: 757.98 kN

% Error = 3.03%

ii) Comparing the obtained value to the reference value from the journal paper,

Authors critical buckling Load: 755.30 kN (from the journal paper [1])

% Difference in the values = 2.687%

4.1.2 Simulation for steel square plates with perforation

4.1.2.1 Overview

A simply support square plate of 1000x1000mm made up of steel grade A36 is used for this study. This plate is subjected to uniaxial loading and the results are obtained for critical buckling stress. The cases solved are for variation of perforation size (i.e. d

=100, 300, 500, 600 and 700mm) and the plate thickness (i.e. t = 10, 11.11, 12.5, 14.286, 16.67, 20, 25 and 33.33mm).

4.1.2.2 Results for hole diameter to plate width (d/b) = 0.1

The square plate for this case has a perforation of 100mm. The critical buckling load is obtained for different plate thickness.

Table 4-1 Result comparison of FEM results to the authors results for d/b = 0.1

Sr No.	b/t	t (mm)	Force (N)	σ_{cr} (MPa)	σ_{cr} / σ_y (FEM)	σ_{cr} / σ_y (Author[2])
1	30	33.33	7.431 e 6	226.65	0.91	0.91
2	40	25	5.6217 e 6	230.52	0.92	0.9
3	50	20	3.7915 e 6	205.84	0.83	0.85
4	60	16.67	2.75 e 6	173.747	0.7	0.74
5	70	14.286	1.864 e 6	136.51	0.55	0.59
6	80	12.5	1.3124 e 6	106.7	0.43	0.45
7	90	11.11	9.195 e 6	81.909	0.330	0.35
8	100	10	6.7225 e 5	79.4	0.27	0.32

4.1.2.3 Results for hole diameter to plate width (d/b) = 0.2

The square plate for this case has a perforation of 200mm. The critical buckling load is obtained for different plate thickness.

Table 4-2 Result comparison of FEM results to the authors results for d/b = 0.2

Sr No.	b/t	t (mm)	Force (N)	σ_{cr} (MPa)	σ_{cr} / σ_y (FEM)	σ_{cr} / σ_y (Author[2])
1	30	33.33	6.6038 e 6	206.52	0.832	0.83
2	40	25	4.993 e 6	202.75	0.81	0.8
3	50	20	3.785 e 6	175.54	0.71	0.75
4	60	16.67	2.556 e 6	155.72	0.63	0.65
5	70	14.286	1.842 e 6	133.02	0.54	0.55
6	80	12.5	1.243 e 6	99.814	0.402	0.43
7	90	11.11	8.739 e 5	77.959	0.31	0.34
8	100	10	6.353 e 5	62.3	0.251	0.28

4.1.2.4 Results for hole diameter to plate width (d/b) = 0.4

The square plate for this case has a perforation of 400mm. The critical buckling load is obtained for different plate thickness.

Table 4-3 Result comparison of FEM results to the authors results for d/b = 0.4

Sr No.	b/t	t (mm)	Force (N)	S_{cr}(MPa) (FEM)	S_{cr} / S_y (FEM)	S_{cr} / S_y (Author[2])
1	30	33.33	4.995 e 6	152.65	0.61	0.6
2	40	25	3.73 e6	151.78	0.611	0.595
3	50	20	2.947 e 6	145.67	0.587	0.58
4	60	16.67	2.04087 e 6	140.54	0.566	0.545
5	70	14.286	1.78026 e 6	120.81	0.487	0.46
6	80	12.5	1.23 e 6	93.638	0.377	0.35
7	90	11.11	8.725 e 5	74.05	0.298	0.29
8	100	10	6.348 e 5	59.538	0.24	0.25

4.1.2.5 Results for hole diameter to plate width (d/b) = 0.5

The square plate for this case has a perforation of 500mm. The critical buckling load is obtained for different plate thickness.

Table 4-4 Result comparison of FEM results to the authors results for d/b = 0.5

Sr No.	b/t	t (mm)	Force (N)	σ_{cr} (MPa)	σ_{cr} / σ_y (FEM)	σ_{cr} / σ_y (Author[2])
1	30	33.33	4.2635 e 6	95.14	0.383	0.4
2	40	25	3.097 e 6	95.067	0.385	0.4
3	50	20	2.486 e 6	96.408	0.388	0.395
4	60	16.67	2.0565 e 6	94.347	0.38	0.39
5	70	14.286	1.7541 e 6	93.895	0.378	0.35
6	80	12.5	1.3108 e 6	76.903	0.3098	0.31
7	90	11.11	9.4858 e 5	62.315	0.251	0.25
8	100	10	6.977 e 5	50.664	0.21	0.23

4.1.2.6 Results for hole diameter to plate width (d/b) = 0.6

The square plate for this case has a perforation of 600mm. The critical buckling load is obtained for different plate thickness.

Table 4-5 Result comparison FEM results to the authors results for d/b = 0.6

Sr No.	b/t	t (mm)	Force (N)	σ_{cr} (MPa)	σ_{cr} / σ_y (FEM)	σ_{cr} / σ_y (Author[2])
1	30	33.33	3.3865 e 6	51.54	0.21	0.23
2	40	25	2.5184 e 6	49.753	0.2	0.23
3	50	20	2.0109 e 6	49.535	0.1995	0.23
4	60	16.67	1.6833 e 6	49.914	0.2	0.23
5	70	14.286	1.4388 e 6	49.719	0.2	0.23
6	80	12.5	1.2534 e 6	49.186	0.198	0.22
7	90	11.11	9.684 e 5	44.446	0.18	0.21
8	100	10	8.113 e 5	42.19	0.17	0.2

4.1.2.7 Results for hole diameter to plate width (d/b) = 0.7

The square plate for this case has a perforation of 700mm. The critical buckling load is obtained for different plate thickness.

Table 4-6 Result comparison of FEM results to the authors results for d/b = 0.7

Sr No.	b/t	t (mm)	Force (N)	σ_{cr} (MPa)	σ_{cr} / σ_y (FEM)	σ_{cr} / σ_y (Author[2])
1	30	33.33	27.975	28.048	0.113	0.11
2	40	25	26.821	26.80	0.108	0.11
3	50	20	27.618	27.55	0.111	0.11
4	60	16.67	27.858	27.79	0.112	0.11
5	70	14.286	26.718	26.558	0.107	0.11
6	80	12.5	28.038	28.05	0.113	0.11
7	90	11.11	27.54	27.55	0.111	0.11
8	100	10	26.921	26.806	0.108	0.11

4.1.2.8 Conclusion and Results

The simulation comparisons explains this. The elastic and plastic buckling were experienced in this study. The critical buckling stress increases towards the yield stress as the plate thickness increases from 10mm to 33.33mm.

Figure 4-3 illustrates change in the governing critical stress verses the plate slenderness ratio for different values of perforation size. The critical buckling stress decreases with the perforation size. The graph is similar to the author's graph [2].

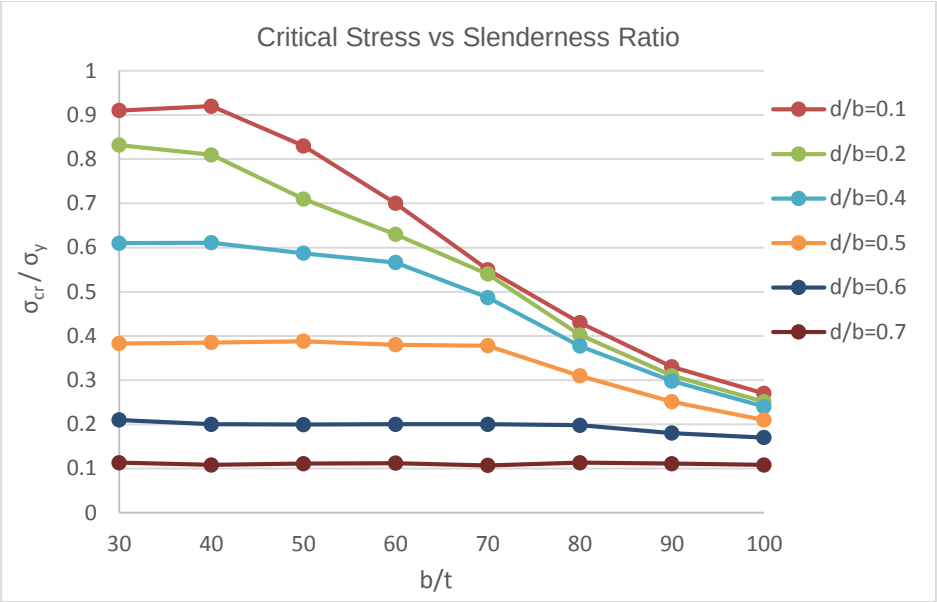

Figure 4-3 Buckling curves for square plate.

4.2 Simulations including strain hardening effect for rectangular plates

4.2.1 Overview

In this case rectangular plates with different aspect ratios are subjected to uniaxial compressive loading. The plate is modeled with some initial imperfection. The plate is clamped on two parallel edges and simply supported on the edges on which the compressive force is applied. The breath of the plate is kept constant i.e. b = 500mm, while the length 'a' is varied from 250 to 2000mm.

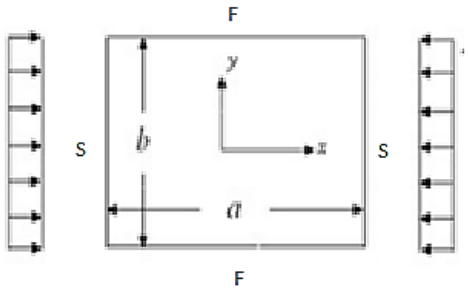

Figure 4-4 Plate under uniaxial loading (F-fixed support, S-simply supported)

The material used is aluminum grade AL 7075-T6. Ramberg-Osgood stress strain curve for c = 2 is used as input in ANSYS. The stress strain curve will define the path of material behavior in the plastic region.

4.2.2 Results for c = 2:

The results are in the form of coefficient of buckling. Which are calculated by using the coefficient of buckling formula [3],

$$K = \frac{\sigma c\, h\, b^2}{D\, \pi^2}$$

Here, *h* is the plate thickness.

Table 4-7 Result comparison of FEM results to the authors results for c = 2

Sr No.	a/b	a (length)	b (breath)	σ_{c-2} (MPa)	K_{c-2} (FEM)	K_{c-2-a} (Authors[3])
1	0.5	250	500	252.74	6.10	6.1
2	1.0	500	500	257.99	6.23	6.2
3	1.5	750	500	267.27	6.4	6.2
4	2.0	1000	500	262.69	6.34	6.1
5	2.5	1250	500	239.52	5.8	6.0
6	3.0	1500	500	245.52	5.9	6.0
7	3.5	1750	500	259.11	6.2	6.1
8	4.0	2000	500	246.65	6.0	6.1

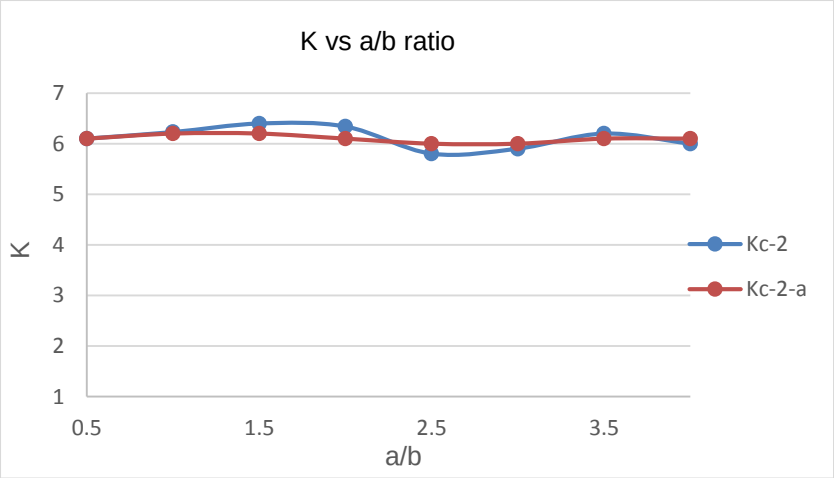

Figure 4-5 Comparison of the FEM buckling coefficient results with the authors [3]

4.2.3 Different Modes of linear elastic buckling for varying aspect ratios.

Table 4-8 demonstrates the different modes of buckling obtained for different aspect ratios

Sr No.	Geometry	Buckling Mode
	250x500x12.5	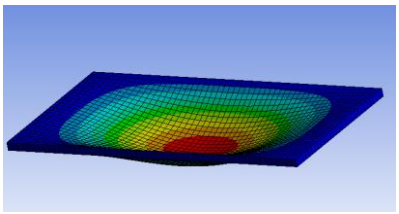 Mode shape - half wave.
2	500x500x12.5	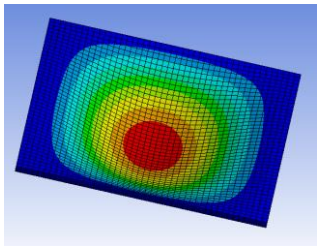 Mode shape - half wave
3	500x750x12.5	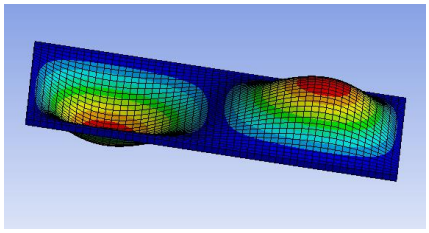 Mode shape – one wave.
4	500x1000x12.5	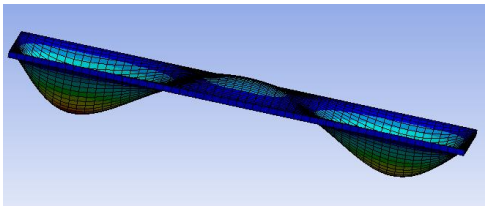 Mode shape - one and a half wave shape

Table 4-8—*Continued*

5	500x1250x12.5	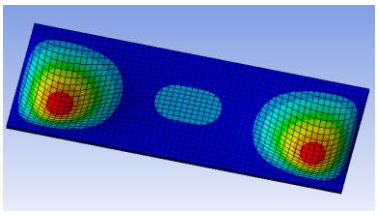 Mode shape - one and a half wave
6	500x1500x12.5	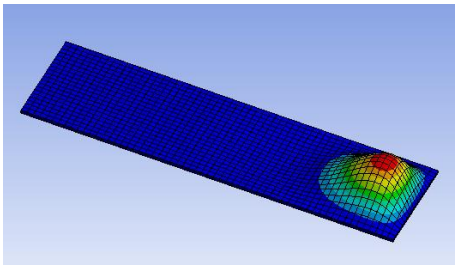 Mode shape - half wave
7	500x1750x12.5	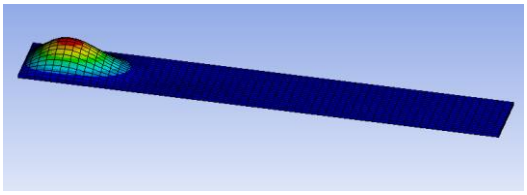 Mode shape - half wave
8	500x2000x12.5	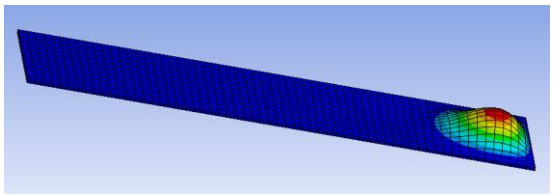 Mode shape - half wave

4.2.4 Results and conclusion

The comparison of the results show that, the results were within the agreeable limits with the author's results. The calculated critical stress in this study does not show a large variation with the change in the aspect ratio as shown in [3].

CHAPTER 5

ANSYS SIMULATION- STRAIN HARDENING EFFECT ON A PERFORATED SQUARE PLATE

In this chapter the buckling behavior for different strain hardening is studied. A plate of 1000x1000mm is simply supported on all four edges and a uniaxial load is applied. The plate is modeled with imperfection in Creo. The FEM analysis is done in ANSYS using static nonlinear for geometric variations. The different cases considered by varying the geometry are,

1) Perforation diameter = 100mm and 700mm
2) Thickness of the plate:

b/t	15	20	30	40	50	60	70	80	90	100
t (mm)	66.66	50	33.33	25	20	16.67	14.286	12.5	11.11	10

Here d/t is the ratio of perforation diameter to plate thickness ratio.

5.1 Material Properties and Inputs

The material used for the plates are AL7075-T6. This aluminum grade is mostly used in transportation, marine, automation and aviation due to high strength to density ratio. The mechanical properties of this grade are,

E (Young's Modulus) = 71700 MPa,

σy (Yield Strength) = 503MPa,

σu (Ultimate Strength) = 570 MPa,

Nu(Poisson's Ratio) = 0.33

The Ramberg-Osgood strain hardening curves are introduced through Multilinear Isotropic hardening in ANSYS.

5.2 Mesh Convergence study

A mesh convergence study is done to select the right size of elements required by the model to ensure that the results of the analysis is not affected by changing the size of the mesh. In the mesh convergence study the critical result parameters is plotted against the mesh density.

In the present study, plates are messed on the basis of their thickness. Thin plates, are meshed with 8-node shell elements. When the plate thickness becomes large the plate is meshed with solid elements. In this case plates with thickness of 33.33, 50 and 66.66mm are meshed with solid elements.

5.2.1 Plate with d/b = 0.1, t = 10mm

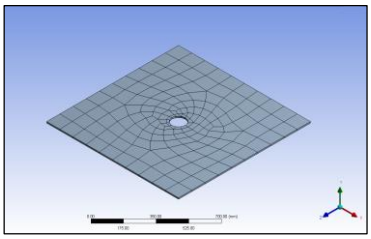

a) 165 shell elements

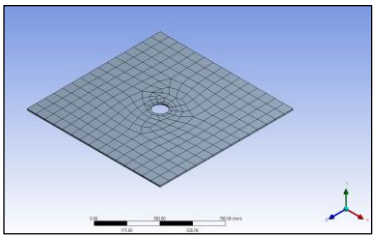

b) 270 shell elements

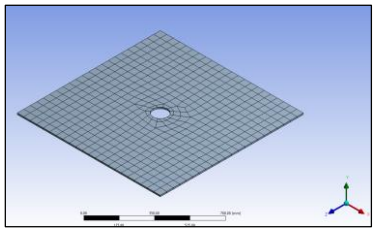

c) Coarse Mesh: 499 shell elements

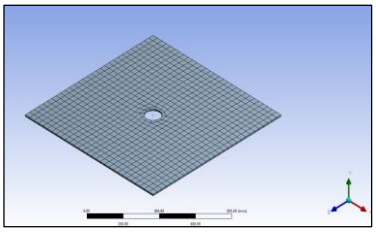

d) Medium Mesh: 844 Shell elements

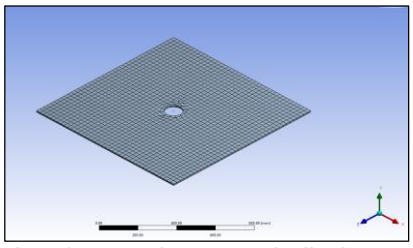

e) Fine Mesh: 1597 Shell Elements

Figure 5-1 Mesh convergence study for plate with d/b = 0.1, t = 10mm.

The plate is meshed from coarse to fine elements and the results for force reaction are found out for each case. This is further explained from the table and graphs provided below.

Table 5-1 The force output results with the variation of no. of elements for d/b = 0.1, t = 10mm.

Sr No.	No. of Elements	Force(N)
1	165	85559
2	270	85558
3	499 (Coarse Mesh)	85558
4	844 (Medium Mesh)	85557
5	1597 (Fine Mesh)	85558

We can see here the elements are refined from 528 to 2815 elements by manually meshing the plate. It is observed that the total change is the force output results is 0.0023 % for the above used plate.

5.2.2 Plate with d/b = 0.1, t = 66.66mm

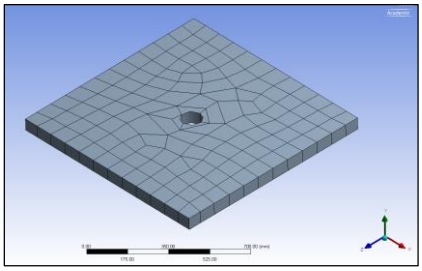

1) 136 solid elements

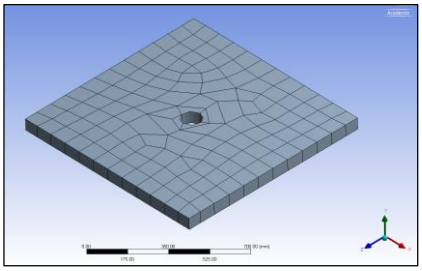

2) 201 solid elements

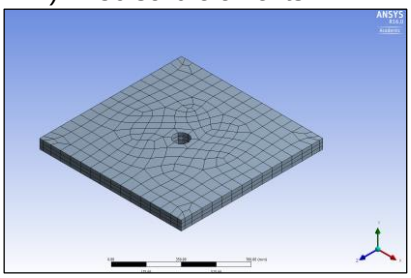

3) Coarse Mesh: 729 shell elements

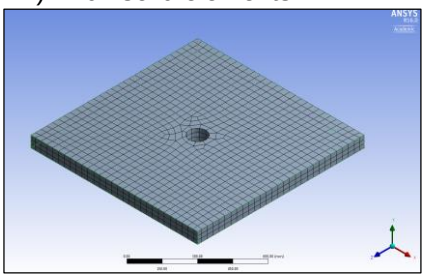

4) Medium Mesh:2496 Solid elements

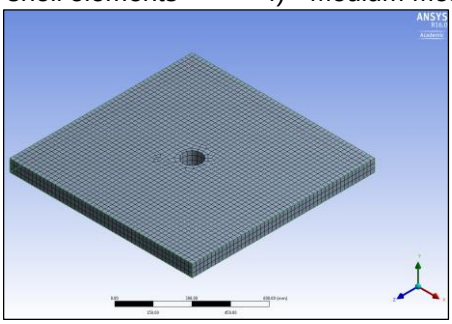

5) Fine Mesh: 6882 Solid Elements

Figure 5-2 Mesh convergence study for plate with d/b = 0.1, t = 66.66mm.

Table 5-2 The force output results with the variation of no. of elements for d/b = 0.1, t = 66.66mm.

Sr No.	No. of Elements	Force(N)
1	136	3.4375e7
2	201	3.4307e7
3	729 (Coarse Mesh)	3.4299e7
4	2496(Medium Mesh)	3.4272e7
5	6882(Fine Mesh)	3.4263e7

Mesh convergence study for plate with solid elements, referning the table given above.

We can see here the elements are refined from 136 to 6882 elements manually. Total change is the force output results is -0.336 %.

5.2.3 Plate with d/b = 0.7, t = 10mm

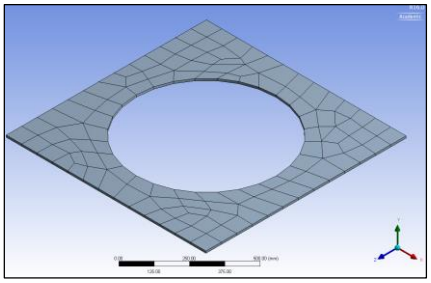

1) 109 Shell elements

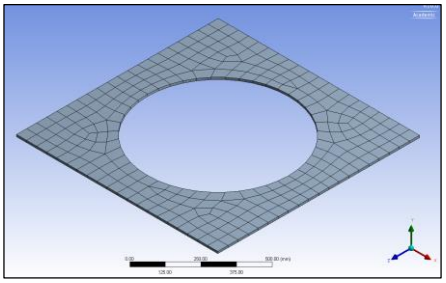

2) 257 Shell elements

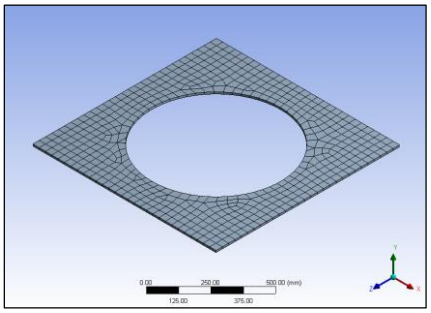

3) Coarse Mesh: 528 Shell Elements

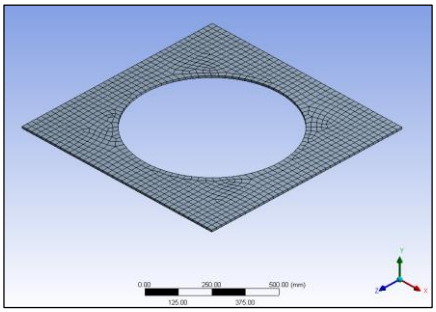

4) Medium Mesh: 1003 Shell Elements

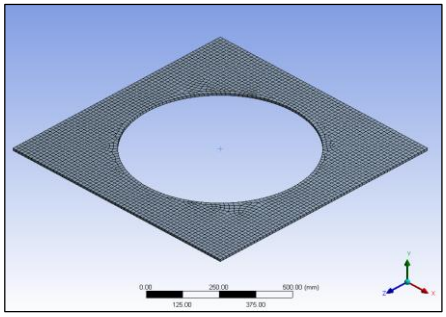

5) Fine Mesh: 2815 Shell Elements

Figure 5-3 Mesh convergence study for plate with d/b=0.7,t=10mm.

Table 5-3 The force output results with the variation of no. of elements for d/b = 0.7, t = 10 mm.

Sr No.	No. of Elements	Force(N)
1	109	1.2772e5
2	257	1.2685e5
3	528 (Coarse Mesh)	1.2622e5
4	1003 (Medium Mesh)	1.2590e5
5	2815 (Fine Mesh)	1.2570e5

Mesh convergence for plate with shell elements, referning the table given above.

We can see here the elements are refined from 109 to 2815 elements manually. Total change is the force output results is -1.607%.

5.2.4 Plate with d/b = 0.7, t = 66.66mm

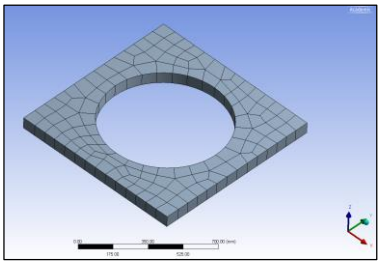

1) 122 solid elements

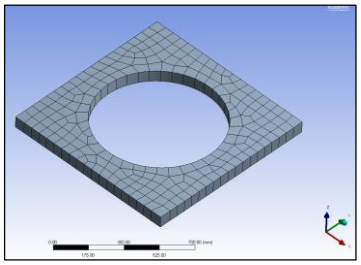

2) 208 solid elements

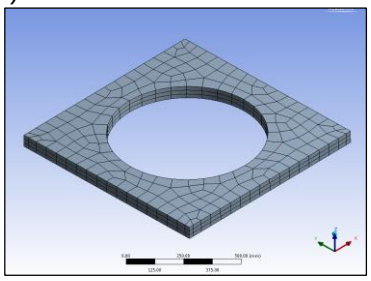

3) Coarse Mesh: 516 solid elements

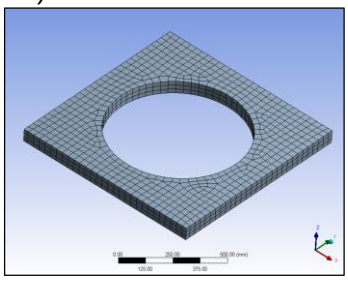

4) Medium Mesh:1632 Solid elements

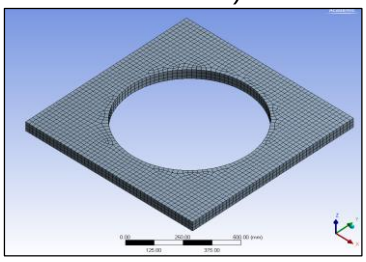

5) Fine Mesh: 4431 Solid Elements

Figure 5-4 Mesh convergence study for plate with d/b = 0.7, t = 66.66mm.

Table 5-4 The force output results with the variation of no. of elements for d/b = 0.7, t = 66.66mm.

Sr No.	No. of Elements	Force(N)
1	122	1.4794e7
2	208	1.4803e7
3	516 (Coarse Mesh)	1.4852e7
4	1632 (Medium Mesh)	1.5048e7
5	4431 (Fine Mesh)	1.5051e7

Mesh convergence for plate with solid elements, referning the table given above.

We can see here the elements are refined from 122 to 4431 elements. Total change is about 1.708% in the output value.

5.2.5 Conclusion

The study of mesh convergence was helpful in selecting the mesh density for each case.

5.3 Boundary conditions

The plate is simply supported and a compressive displacement is applied along the edges. Equivalent force value for this applied displacement is obtained through force reaction results.

5.3.1 For Thin plates:

The plate is simply supported on all of its edges, i.e. y = 0

And a compressive displacement is applied along X axis.

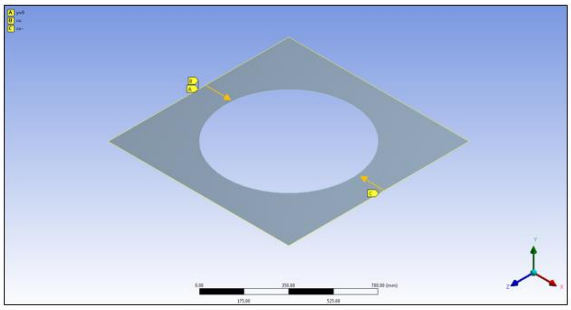

Figure 5-5 Boundary Condition for thin plates

5.3.2 For Thick plates:

The plate is simply supported at the lower face edges, i.e. z = 0

And a force a uniaxial load is applied to the surface along X axis.

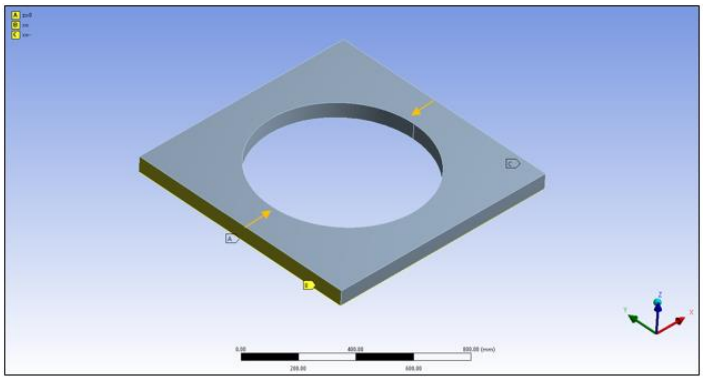

Figure 5-6 Boundary Condition for thick plates

5.4 Results

5.4.1 Total deformation

Total deformation provide us with the direction in which the plate will deform.

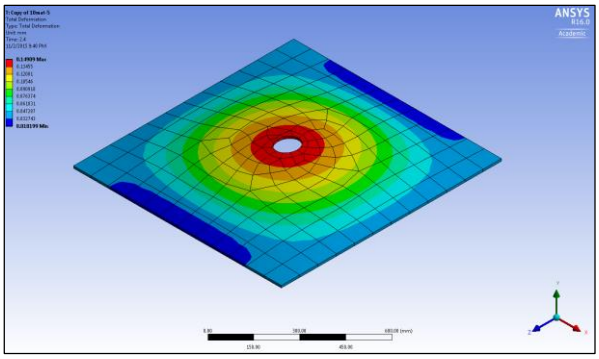

Figure 5-7 total Deformation of perforated plate

The results are magnified to see the deformation of the body. It can be seen that the plate deflects in X direction due to uniaxial loading.

5.4.2 Linear Elastic Buckling

The linear elastic buckling provides use with the load magnitude causes the buckling modes, in the form of load multiplier. Also it helps us predict the buckling mode.

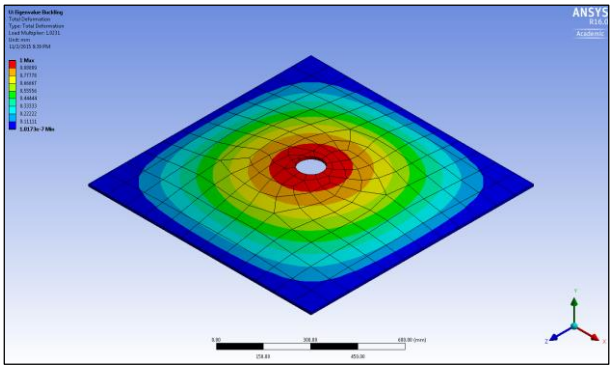

Figure 5-8 Eigen value Buckling

Here the load multiplier is almost 1, which tells us that the applied load is the buckling load for this mode shape as shown in Figure 5-8.

5.4.3 Buckling results for different slenderness ratio

Bucking is elastic for plate with small thickness and perforation. As the perforation size and thickness increases the buckling changes from elastic to elasto-plastic.

5.4.3.1 Results for c = 5, 10, 20 and d/b = 0.1

Table 5-5 Compares the critical stress buckling results for c-5, 10, 20 and d/b = 0.1

b/t	t (mm)	σ_{c-5} (MPa)	σ_{c-10} (MPa)	σ_{c-20} (MPa)	Difference (%)
100	10	8.969	8.7257	8.986	2.890
90	11.11	10.811	10.517	10.831	2.899
80	12.5	13.948	13.59	13.973	2.740
70	14.286	17.39	16.917	17.421	2.893
60	16.67	24.205	23.546	24.248	2.895
50	20	34.214	33.283	34.278	2.902
40	25	54.162	52.689	54.259	2.890
30	33.33	157.59	153.26	157.83	2.895
20	**50**	**330.4**	**343.58**	**345.21**	**4.290**
15	**66.66**	**380.1**	**381.07**	**398.62**	**4.646**

Highlighted values show the elasto-plastic behavior.

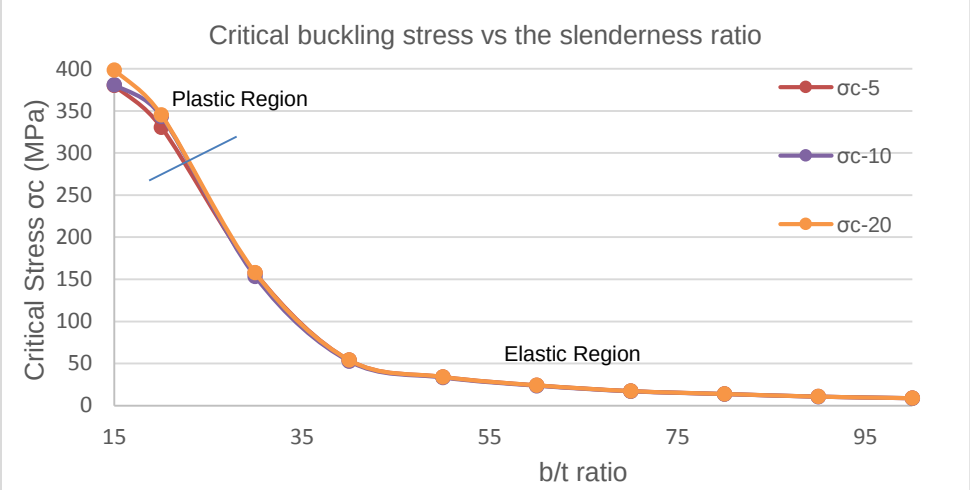

Figure5-9 comparison of different critical stress values obtained for strain hardened cases for various slenderness ratio (d/b = 0.1).

From the graph we can say the values are almost in sync till the slenderness ratio is 20, i.e. t = 50. After this point some variation in the results is seen for different strain hardening curves. The maximum difference in the critical buckling stress for different strain hardening is 4.646%.

5.4.3.2 Results for c = 5, 10, 20 and d/b = 0.7

Table 5-6 Compares the critical stress buckling results for c-5, 10, 20 and d/b = 0.7

b/t	t (mm)	$\sigma_{c\text{-}5}$ (MPa)	$\sigma_{c\text{-}10}$ (MPa)	$\sigma_{c\text{-}20}$ (MPa)	Difference (%)
100	10	41.578	40.449	41.652	2.880
90	11.11	51.223	49.832	51.314	2.880
80	12.5	62.521	60.831	62.632	2.875
70	14.286	83.128	80.881	83.276	2.876
60	16.67	111.45	108.44	111.65	2.701
50	20	159.94	155.86	160.38	2.818
40	25	238.88	240.157	244.3	2.218
30	**33.33**	**314.55**	**326.78**	**328.26**	**4.176**
20	**50**	**311.91**	**322.27**	**325.37**	**4.136**
15	**66.66**	**326.22**	**339.45**	**342.34**	**4.709**

Highlighted values show the elasto-plastic behavior.

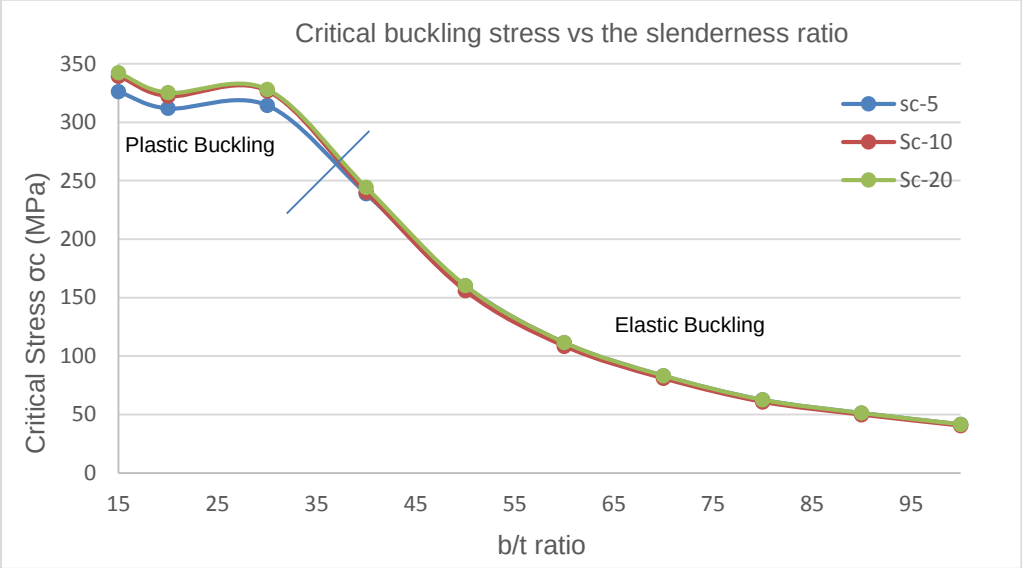

Figure 5-10 comparison of different critical stress values obtained for strain hardened cases for various slenderness ratio (d/b = 0.7).

From Figure 5-10 we can say the values are almost in sync till the slenderness ratio is 30, i.e. t = 33.33. After this point some variation in the results are seen with different strain hardening curves. The maximum difference in the results seen in this case are 4.709% in the critical stress value.

5.4.4 Stresses in the plastic region

In this part the results for elasto-plastic buckling are shown. The plate with large thickness and perforation are considered.

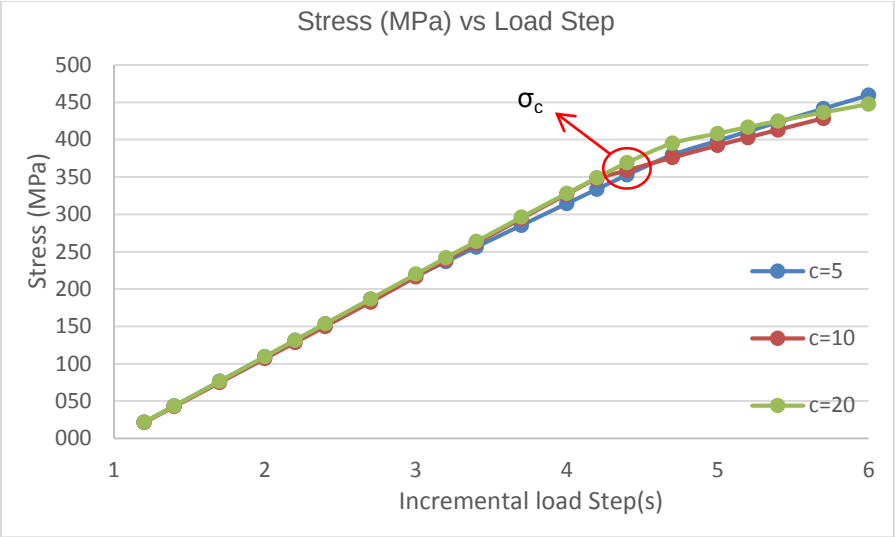

Figure 5-11 Graph for normal stress vs incremental load step(s) for c = 5, 10, 20 and t = 33.33mm and b/d = 0.7

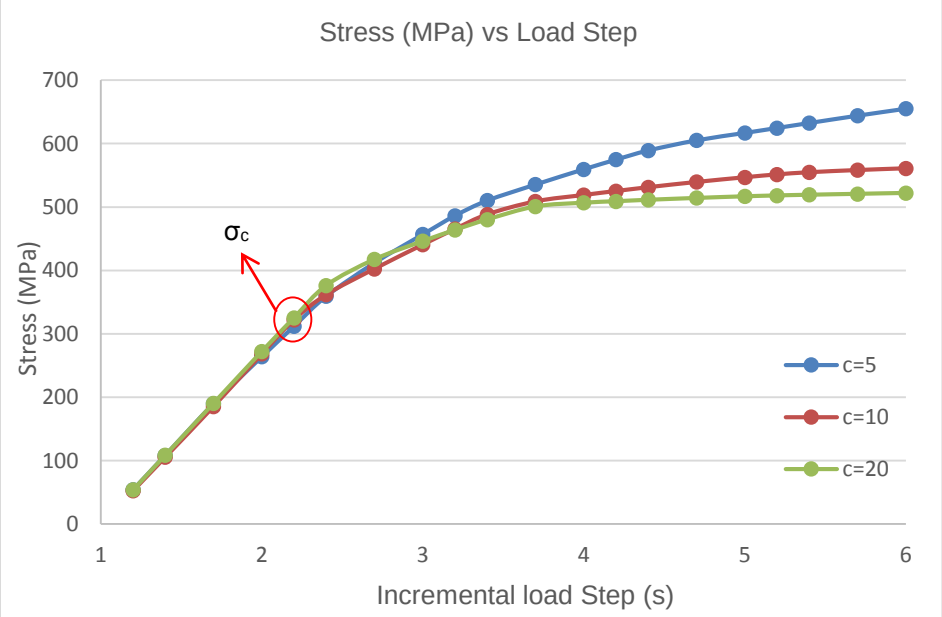

Figure 5-12 Graph for normal stress vs incremental load step(s) for c = 5, 10, 20 and t = 50mm and b/d = 0.7

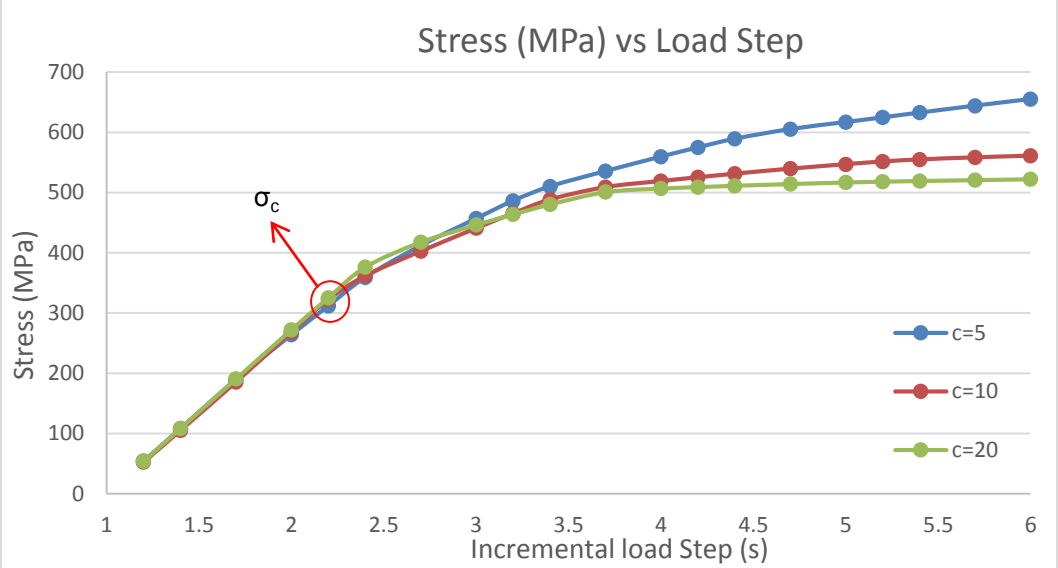

Figure 5-13 Graph for normal stress vs incremental load step(s) for c = 5, 10, 20 and t = 66.66mm and b/d = 0.7

From the three plots it could be seen that as the thickness of the plate increases there is a large variation in the stress values in the plastic region. In the Figure 5-11 the plate thickness is 33.33mm and the variation in the stress values is seen after the point of critical buckling stress. As the thickness increases till 66.66mm (shown in Figure 5-13) a large variation in the results is seen in the plastic region.

CHAPTER 6

CONCLUSION & FUTURE WORK

6.1 Conclusion

i. For the cases considered here, it is seen that the critical buckling stress is lower than the yield strength. Hence the maximum amount of variation in the results of critical buckling stress for different strain hardening cases of c = 5, 10 and 20, is seen to be 4.7%.

ii. The variation in the results of critical buckling stress for different strain hardening cases of c = 5, 10 and 20, is seen for thick plates.

iii. There is a large variation in the results of critical buckling stress for different strain hardening cases of c = 5, 10 and 20 seen in the elastic-plastic region.

6.2 Future Work.

i. The study was done for the grade AL 7075. Further the study could be made for different materials like steel or Magnesium.

ii. The strain hardening method was used defining the plastic region through Ramber-Osgood stress strain curve. The study could be conducted using different strain hardening model.

iii. The study could also be conducted for different shapes and locations of the perforation.

REFERENCES

[1] Real, M. D. V.; Isoldi, L. A.; Damas, A. P.; Helbig, D.; 'Elastic and Elasto-Plastic buckling analysis of perforated steel.' *Vetor, Rio Grande, v. 23, n. 2, p. 61-70, 2013*

[2] El-Sawy, K. M.; Nazmy, A. S.; Martini, M. I. 'Elasto-plastic buckling of perforated plated under uniaxial compression', *Thin-Walled Structure, v.42,p.122-133,2007.*

[3] Maarefdoust, M.; Kadkhodayan, M.; 'Elastoplastic buckling analysis of rectangular thick plates by incremental and deformation theories of plasticity', *Proc IMechE Part G: J Aerospace Engineering, v.229 (7), p. 1280–1299, 2015.*

[4] Paik, J.K. ; 'Ultimate strength of perforated steel plates under combined biaxial compression and edge shear loads', *Thin-Walled Structure, v. 46, p. 207-213,2008.*

[5] Brown, C. J.; Yettram, A. L.; 'The elastic stability of square perforated plates under combination of bending, shear and direct load.' *Thin-Walled Structures, v.4 (3).p.239–46, 1986.*

[6] Durban, D.; Zuckerman, Z; 'Elastoplastic buckling of rectangular plates in biaxial compression/ tension.*' International Journal of Mechanical Science, v.41.p.751–65, 1999.*

[7] Shakerle, T. M.; Brown, C. J.; 'Elastic buckling of plates with eccentrically positioned rectangular perforation', *International Journal of Mechanical Science, v.38 (8–9), p.825–38, 1996.*

[8] Timosheko; Gere; 'Theory of Elastic Stability', *second edition, McGraw-Hill Book Company, New York, p. 348-456 ,1961.*

[9] Ramberg Osgood (https://en.wikipedia.org/wiki/Ramberg%E2%80%93Osgood_relationship)

[10] Material Data sheet for Al7075 (http://asm.matweb.com/search/SpecificMaterial.asp?bassnum=MA7075T6)

[11] Mesh convergence (http://www.nafems.org/join/resources/knowledgebase/001/)

[12] Local Buckling

(https://www.princeton.edu/~maelabs/mae324/glos324/plasticbuckling.htm)

BIOGRAPHICAL INFORMATION

Mayuri Patil (1989), obtained her Master's in Mechanical Engineering in December 2015 from The University of Texas at Arlington. She completed her Bachelor's Degrees in Mechanical Engineer in 2011 from Pune University, India.

While she was an undergraduate student, she was a part of a runner up team which stood 2nd over 80 teams at a national level event at SAE Baja 2011-India. She was associated with 'The Automotive Research Association of India', as a Project Engineer at the CAE Dept. She was a part of the project related to 'Design guideline for light weighting of seat for city bus application '. Here her work was related to modeling and Finite Element Analysis using hyper-mesh and LS-dyna for crash analysis.

During her graduate career she served as a Graduate Teaching Assistant for Dr. Kent Lawrence. Her thesis was related to static-structural, non-linear analysis related .Her current research interests are in the field of Computer Aided Engineering and Computational Geometry.